Q. J. R. Meteorol. Soc. (1997), **123**, pp. 467–489

A Lagrangian-based analysis of extratropical cyclones. I: The method and some applications

By HEINI WERNLI* and HUW C. DAVIES
ETH Zürich, Switzerland

(Received 13 February 1996; revised 31 May 1996)

SUMMARY

A Lagrangian-based method of analysis is introduced to examine the space–time structure and dynamics of extratropical cyclogenesis. The three-step method involves the calculation of extensive ensembles of trajectories, the evaluation of the Lagrangian time-trace of physical variables along these paths, and the application of objective selection criteria to identify significant Lagrangian structures. The approach can provide a qualitative depiction of, quantitative information about, and dynamical insight into, key features of mid-latitude cyclones. In this, the first of a two-part study, examples are given of the application of the method. A case-study approach has been adopted and used to identify coherent ensembles of trajectories (CETs) whose dynamics are seminal to an event of Atlantic cyclogenesis, to trace the origin of subsynoptic potential vorticity anomalies, and to analyse stratosphere–troposphere exchange accompanying extratropical cyclogenesis. In addition, a statistical investigation has been made of the climatology of CETs in the northern hemisphere for one particular winter month. Some consideration has been given to the shortcomings and potential of the method, and its complementarity with other approaches.

KEYWORDS: Lagrangian climatology North Atlantic cyclogenesis Potential-vorticity anomalies Trajectory ensemble Tropopause–stratosphere exchange

1. INTRODUCTION

In the study of synoptic scale atmospheric motion it has been customary to adopt an Eulerian, as opposed to a Lagrangian, framework. The Eulerian framework with its spatially fixed coordinates conforms to most observing systems. It is also a practicable framework for the analysis and diagnosis of the pertinent flow systems, fronts, cyclones and anticyclones, since these possess distinctive, spatially coherent structures that evolve smoothly with time. In contrast the Lagrangian scheme is geared to asynoptic non-routine measurements that track the airflow; moreover during cyclogenesis the Lagrangian specification of the flow can evolve to an intricate and convoluted form. There is therefore less documentation and more uncertainty regarding the existence of temporally coherent Lagrangian structures within mid-latitude cyclones.

Nevertheless the Lagrangian frame is physically more meaningful and significant insight has been gained from the extant Lagrangian-based studies. Early study of surface measurements (e.g. Dove 1840; Fitzroy 1863) pointed to the existence of distinct air currents and airmasses within synoptic systems. Analysis of the path of an isolated volume of air (a macro air-parcel), and calculations of surface trajectories associated with low pressure systems (Shaw 1903; Shaw and Lempfert 1906) served to emphasize the presence of distinct airmasses and revealed significant bands of convergence and divergence. These same Lagrangian notions also featured prominently in the development of the classical Bergen frontal model.

Later isentropic analyses of the airflow relative to the translating synoptic system provided evidence of the existence of dry descending, and moist ascending, tongues of air within cyclones and anticyclones (Rossby *et al.* 1937; Namias 1939). The upper-troposphere descending tongues often assume a hammer-head shape to the west of the developing surface cyclone (e.g. Rossby 1945; Palmén 1953; Danielsen 1980; Young *et al.* 1987). Likewise detailed analysis of the ascending tongues indicates that they acquire

* Corresponding author: Institute for Atmospheric Science, ETH Hönggerberg, CH-8093 Zürich, Switzerland. e-mail: wernli@atmos.umnw.ethz.ch.

a narrow elongated form characterized by a zone of rapid relative movement (Green *et al.* 1966; Harrold 1973; Browning and Mason 1981). At low levels the tongues are located ahead of the cold and warm fronts and, in accord with their properties, have been termed, respectively, the warm and cold conveyor belts. Further refinements of these concepts include the distinction between rearward-sloping and forward-sloping warm conveyor belts, and the recognition that the upper dry descending tongue can reach very low elevations or overrun the surface cold front. A glossary and synthesis of these pseudo-Lagrangian concepts has been provided by Browning and Roberts (1994) and overviewed by Browning (1990, 1995).

Validation of the conveyor-belt structures is difficult. A filamentary structure on a single isentropic chart equates directly to a comparable Lagrangian flow pattern only if the system is in uniform translation and steady. In effect observational verification requires an adequate Lagrangian data-set derived by recasting Eulerian data derived from either observational measurements or a numerical model simulation.

At present there is a dichotomy in the status of the conveyor-belt studies. On the one hand their synthesis has led to the creation of 'structure models' (Carlson 1991; Browning 1995; Bader *et al.* 1995) that are useful in the interpretation of satellite and radar imagery of a system's cloud and precipitation patterns. In addition Schär and Wernli (1993) diagnosed spatially confined Lagrangian features consistent with the presence of conveyor belts in an idealized model study of cyclogenesis. On the other hand the suitability of the structure models has been called into question by studies of some individual cyclogenesis events (Kuo *et al.* 1992; Mass and Schultz 1993). The latter studies included the evaluation of a large number of subjectively selected backward trajectories, and revealed complex flow structures not immediately interpretable in terms of conveyor belts.

In this two-part study we adopt a case-study approach and an avowedly Lagrangian perspective. The aim is to explore the existence and nature of key flow structures of extratropical cyclogenesis as portrayed in this framework. The ancillary objectives are to shed light on the conveyor-belt hypothesis, and to complement the understanding gained using traditional synoptic analysis techniques and the potential-vorticity (PV) perspective (Hoskins *et al.* 1985).

In Part I the main goal is to introduce the proposed Lagrangian-based method of analysis and to provide brief illustrative examples of its application. A sequence of case-studies, selected to reflect current research themes, are used to examine the occurrence of coherent Lagrangian flow structures (cf. Browning 1995), to investigate the dynamics of subsynoptic-scale elements (cf. Davies 1994; Simmons 1994; Thorpe 1994), and to explore the nature of the tropopause-level processes associated with stratosphere–troposphere exchange (cf. Shapiro and Keyser 1990; Appenzeller *et al.* 1996). In addition a one-month climatology of the coherent Lagrangian features is compiled to ascertain their preferred geographic location and frequency of occurrence.

2. The analysis method

(*a*) *The rationale*

In a Lagrangian framework the flow is described by the position $\mathbf{r}$ of a micro air parcel (or air particle) as a function of its label, $\mathbf{s}$, and time, τ, i.e. $\mathbf{r} = \mathbf{r}(\mathbf{s}, \tau)$. Here the label is taken to refer to its spatial location at a stipulated reference time. Thus this framework moves with the individual air parcels, and the description of the flow consist in

(i) the identification of the spatial coordinates and physical properties of the air parcels at the reference time,

(ii) the time-trace of the location and physical properties of the same air parcels for prior and/or subsequent time periods.

For synoptic-scale flow the key physical variables are the potential temperature (conserved under adiabatic conditions), the wet-bulb potential temperature (conserved under adiabatic as well as moist adiabatic conditions) and the potential vorticity (conserved for adiabatic, inviscid flow). On timescales comparable with the growth of synoptic-scale systems (approx. 2 days) the influence of three-dimensional deformation effects will, in general, severely distort and convolute a macro air parcel (i.e. an ensemble of neighbouring air parcels) and non-conservative effects, particularly turbulent cloud-diabatic and planetary boundary-layer processes, will result in an air parcel losing its original physical identity.

Here we seek to devise a Lagrangian-based diagnostic analysis scheme formulated around the foregoing features, and to highlight the challenge recall that an Eulerian-based time sequence of conventional synoptic charts serves, in effect, to identify the evolution with time of organized spatial structures within extratropical cyclones. By analogy, the Lagrangian scheme should help in detecting the existence, and diagnosing the origin and nature of the spatial evolution of temporally coherent flow structures within these systems. Coherence of a Lagrangian feature will also signify its dynamical importance if its path brings it into the proximity of the cyclone centre, and if its physical characteristics connote anomalous values of potential vorticity and/or significant condensation-related changes to the potential temperature and moisture content.

(*b*) *The strategy*

Here we outline a strategy for detecting coherent Lagrangian flow structures and for indicating their potential importance. In it we have built upon the technique introduced by Schär and Wernli (1993); it is designed to operate with a sequence of either analysis fields from an operational NWP assimilation–analysis suite or the space–time fields from a numerical model simulation.

The method consists of a series of three linked steps. First a large number of (forwards or backwards) air-parcel trajectories are calculated for a certain time period (typically 48 hours). These trajectories are chosen to start from every model gridpoint within some predefined three-dimensional domain whose size and location depends upon the specific application (e.g. the North Atlantic (Europe) for the case-studies described in section 3(a) and (c), a dynamically prescribed limited volume in section 3(b), and the entire northern hemisphere for the climatological analysis in section 4). The resulting trajectories number between 1000 and 250 000. For each trajectory time traces are determined for the horizontal and vertical position (longitude, latitude, pressure), the potential and wet-bulb potential temperature (θ, θ_w), the specific and relative humidity (q and RH) and the potential vorticity (PV). These data are stored at intervals of 1 hour.

In a further step a limited ensemble of trajectories is selected from this large pool depending on one (or more) specific dynamically based criterion. The three types of criteria can be classified as follows:

(i) *A priori* criteria based upon the spatial coordinates and physical properties of the air parcels at the reference time. One such criterion is the selection of the trajectories describing macro air parcels that emanate from a domain characterized at the reference time by values of a field variable (e.g. potential vorticity) that exceed, or fail to exceed, a specified threshold (say, 1 PVU)*. Such a criterion can, in principle, yield

* potential-vorticity unit.

the pre- or antecedent trace of a dynamically pertinent element such as a low-level positive potential vorticity anomaly or a mid-level moist tongue.

(ii) *A posteriori* criteria based upon the time trace either of the air-parcel paths (e.g. significant ascent or descent during a certain time interval) or of the physical characteristics along the path (e.g. significant increase of potential temperature or potential vorticity, or significant decrease of specific humidity); each criterion requires the specification of a threshold value for significance. In effect this procedure can result in the objective selection of coherent ensembles of trajectories (CETs) that represent distinctive macro air parcels.

(iii) A combination of *a posteriori* and *a priori* criteria such as, for example an *a priori* constraint to identify stratospheric air (say potential vorticity values greater than 2 PVU at high elevations) and an *a posteriori* constraint of significant descent. This combination will trace stratospheric intrusions into the troposphere. A replacement of the *a posteriori* constraint by one that requires the air parcels to attain values of less than 2 PVU will serve to select air parcels that traverse the tropopause during the specified time period.

The analysis and illustration of the selected ensemble of trajectories is facilitated by projecting its spatial trace onto a stereographic map (cf. Fig. 2), and summarizing the ensemble-mean values of key physical variables (cf. Table 1).

(*c*) *The data-set and trajectory calculations*

The data-base for the present study is the initialized analysis fields of the ECMWF (European Centre for Medium-Range Weather Forecasts) operational global assimilation scheme. These data are derived with the T213 L31 model (see e.g. Simmons 1991) and provide a consistent state-of-the-art data-set that is available with a time resolution of 6 hours. For the present purposes the required fields (temperature, T; specific humidity, q; surface pressure, p_s; and the three wind components u, v and ω) are interpolated onto a regular latitude–longitude grid with a grid spacing of (usually) 0.75° corresponding in mid latitudes approximately to 85 km in longitude and 60 km in latitude.

In addition, values are derived for the aforementioned set of secondary diagnostic variables (relative humidity, RH; potential temperature, θ; wet-bulb potential temperature, θ_w; potential vorticity, PV; and the diabatic heating rate attributable to the resolvable-scale condensation, $\dot{\theta}_c$). The latter variable was evaluated, following the approach used by Berrisford (1988) who assumed that condensation occurred where ascending air is (nearly) saturated (see Wernli (1995) for details).

The kinematic evaluation of the trajectories was undertaken with a variant of Petterssen's (1956) method, used also in the recent studies by Whitaker *et al.* (1988), Kuo *et al.* (1992) and Reed *et al.* (1992). The position vectors, $\mathbf{r}$, of trajectories that emanate from the original regular spatial grid at the reference time are evaluated with a predictor–corrector procedure that comprises a forward time-step,

$$\mathbf{r}^{*n+1} = \mathbf{r}^n + \mathbf{v}(\mathbf{r}^n) \cdot \Delta t,$$

followed by successive (order of 3) iterations performed with an adjusted mean wind,

$$\mathbf{v}^* = 1/2\,\{\mathbf{v}(\mathbf{r}^n) + \mathbf{v}(\mathbf{r}^{*n+1})\}.$$

The requisite wind components at the intergrid locations are again derived by linear interpolation of the gridded values. The half-hour time-step is consistent with Seibert's (1993) assessment of the accuracy of the Petterssen method for a time data resolution of 6 hours, but this time resolution is itself only marginally adequate, at least for rapidly deepening cyclones (Doty and Perkey 1993).

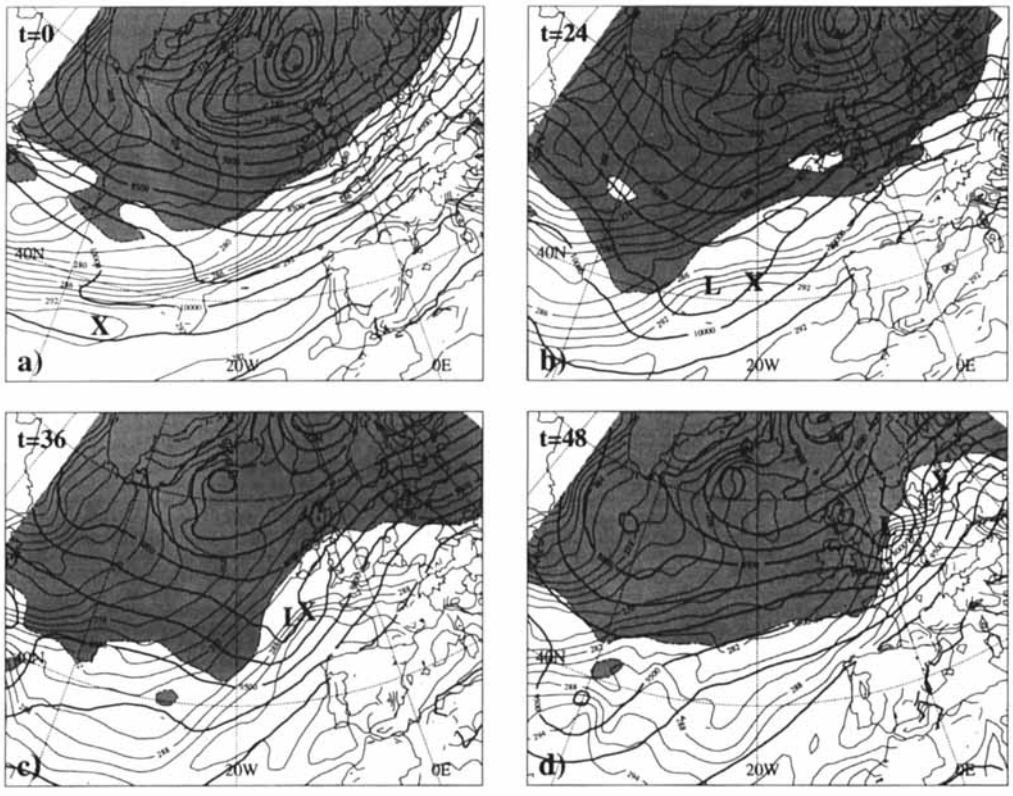

Figure 1. The geopotential pattern (bold lines, contour interval 500 $m^2 s^{-2}$) and the potential temperature field (continuous lines, interval 2 K) on the 900 hPa surface at (a) 18 UTC 11 January, (b) 18 UTC 12 January, (c) 06 UTC 13 January and (d) 18 UTC 13 January 1993. The shaded area corresponds to potential vorticity $\geqslant$ 2 PVU on 315 K. The label **L** denotes the position of the cyclone centre, and **X** corresponds to the actual position of the CET shown in Fig. 2(a).

3. Some case-study applications

(*a*) *Identification of a Lagrangian feature*

A case-study analysis has been done to establish the existence and identify the nature of a Lagrangian feature associated with an event of moderate cyclogenesis that occurred over northern Europe in January 1993. At the surface the development occurred as an upper-level trough propagated towards an elongated and strong low-level baroclinic zone that extended from the central Atlantic to Scandinavia (see Fig. 1). An incipient cyclone near position 30°W, 40°N, which was evident on the 900 hPa geopotential field at 12 UTC 12 January, reached maturity over southern Finland about two days later. (A synoptic overview and isentropic analysis of the event has been given by Browning and Roberts 1994.)

The reference time and the spatial domain for the Lagrangian analysis is set, respectively, for 18 UTC 11 January and for all model gridpoints below 800 hPa in the sector comprising the North Atlantic and western Europe. Trajectories emanating from this region are then evaluated over the subsequent 48 hours—a time period which includes a phase of moderate deepening of the low-pressure system. Consistent with the earlier discussion we focus on air parcels that experience significant cloud-diabatic effects, and we impose as a discriminator a criterion of a specific humidity decrease greater than 10 g kg^{-1}.

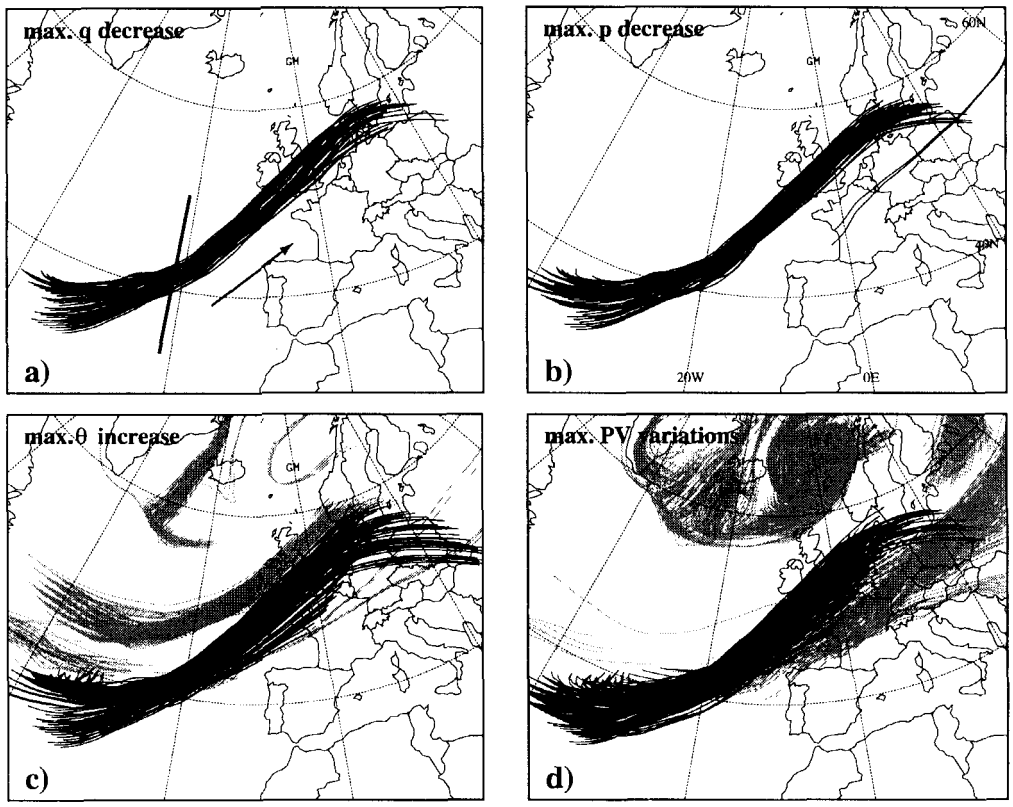

Figure 2. Ensembles of trajectories for the 48 hours interval from 18 UTC 11 January to 18 UTC 13 January 1993, selected with the *a posteriori* criteria of (a) decrease in specific humidity greater than 10 g kg^{-1}, (b) ascent greater than 620 hPa, (c) increase of potential temperature greater than 20 K (and ascent greater than 250 hPa), (d) PV variations (sum of the absolute 6-hourly changes) greater than 2 PVU (and ascent greater than 250 hPa). Trajectories that do not belong to the CET shown in panel (a) are drawn in grey. In panel (a) the arrow indicates the direction of motion, and the bold line marks the location of the vertical section shown in Fig. 3.

The selected trajectories (Fig. 2(a)) reveal a coherent ensemble of trajectories (hereafter referred to as a CET) about 300 km in width that traverses a distance of some 4000 km during the stipulated period. Table 1 summarizes the CET's Lagrangian characteristics. Consider in turn its track and the evolution of its physical characteristics. It originated in the boundary layer of the warm sector somewhat south of the surface front (see Fig. 1(a)), and experienced only modest ascent during the first 18 hours. In a second phase, following the approach of an upper-level PV anomaly and the initiation of surface cyclogenesis at around 18 UTC 12 January (Fig. 1(b)), this macro air parcel rises rapidly by some 500 hPa to the upper troposphere. This narrow updraught region is located close to the translating centre of the evolving low-pressure system (see the labels L and X in Fig. 1(b) and (c)). At the final time the surface cyclone is located just below the front edge of the upper-level trough, and the CET is itself embedded within an upper-level ridge of low potential vorticity that extends as far as latitude 60°N (Fig. 1(d)).

It is in the second phase that the mean properties of the CET exhibit significant changes. Its water-vapour content is depleted by 7.6 g kg^{-1}, its mean potential temperature increases by almost 17 K, and its mean potential vorticity first increases markedly to about 0.8 PVU before decreasing to below its initial reference value. The gradual but slight

TABLE 1. MEAN VALUES AND VARIANCES EVERY 6 HOURS OF THE TRAJECTORY INTEGRATIONS OF THE POSITION (LONGITUDE, LATITUDE, PRESSURE), POTENTIAL TEMPERATURE, θ; WET-BULB POTENTIAL TEMPERATURE, θ_w; POTENTIAL VORTICITY, PV; RELATIVE HUMIDITY, RH; AND SPECIFIC HUMIDITY, q, FOR THE CET SHOWN IN FIG. 2(A).

t [h]	long	lat	p [hPa]	θ [K]	θ_w [K]	PV [PVU]	RH [%]	q [g/kg]
0	-35.0	35.4	981± 9	291.0±0.8	289.4±0.4	0.27±0.1	92± 6	10.8±0.3
6	-32.1	36.3	961±22	292.2±1.0	289.6±0.5	0.37±0.1	91± 3	10.6±0.6
12	-29.0	37.4	932±39	292.6±1.3	288.5±0.7	0.36±0.1	89± 4	9.2±1.1
18	-25.3	39.3	891±63	292.6±2.0	287.4±1.0	0.36±0.2	94± 5	8.1±1.4
24	-21.5	41.5	819±88	294.9±3.6	286.6±1.1	0.64±0.4	94± 5	6.4±1.7
30	-17.0	44.1	697±99	299.1±4.9	285.8±0.8	0.81±0.3	91± 6	4.0±1.6
36	-11.2	47.8	553±96	305.8±4.0	285.8±0.5	0.77±0.4	73± 6	1.8±1.0
42	-1.6	52.8	419±86	309.4±1.8	285.7±0.4	0.42±0.3	53± 9	0.5±0.5
48	13.3	56.0	339±52	309.8±1.2	285.4±0.4	0.12±0.1	56±10	0.2±0.2

Time $t = 0$ corresponds to 18 UTC 11 January 1993.

decrease in the value of the mean wet-bulb potential temperature, θ_w, is attributable to the parametrized heat and moisture fluxes (particularly during the first 18 hours when the parcel translates within the planetary boundary layer), and/or to the inadequacy of the model-derived data-base and the inaccuracies in the calculation of the trajectories.

An alternative way of illustrating the location of the CET relative to the evolving system at a particular time is to display the location of the individual trajectories on a vertical cross-section oriented across the centre of the CET. Figure 3 is one such example and is valid for 18 UTC 12 January. It shows that the trajectories comprising the CET reside within a frontal region characterized by maximum values of the condensational heating. A time-sequence of such sections (not shown) indicates that the individual trajectories ascend through this diabatic heating region and emerge at upper levels. This picture is consistent with the aforedescribed Lagrangian time history of the potential temperature (an increase within the diabatic region) and the potential vorticity (a positive tendency beneath the maximum of heating and a negative tendency above).

The nature of the CET which is identified and discussed above is determined by the starting time (18 UTC 11 January), the time span of the trajectory calculations (48 hours), and the threshold value (10 g kg^{-1}) and nature (specific humidity decrease) of the imposed selection criterion. In the present case, trajectories calculated from different starting times (between 12 UTC 11 January and 12 UTC 12 January) yield similar CETs. Likewise modest variations to the time span and the threshold value, although influencing the number of selected trajectories, do not markedly change the degree of coherence and physical characteristics of the resulting trajectories. Again the application of *a posteriori* selection criteria that require either maximum ascent, or both significant vertical displacement and a maximum potential-temperature increase (or potential-vorticity variations), isolate similar ensembles of trajectories (see Figs. 2(b) to (d)); although the latter two criteria identify not only the considered CET but also other diabatically influenced flow structures (see the trajectories drawn in grey). Thus this CET is distinctive and has a multi-faceted dynamical character.

This dynamical integrity has important implications. First, the inference that this CET is preceded and succeeded by similar features is evidence for the existence of a coherent stream of CETs and a possible conveyor-belt-like flow structure. (An illustration of it can be found in the paper by Wernli (1995), and this issue will be considered in more detail in Part II (Wernli 1997).) Secondly it indicates that this CET, together with its

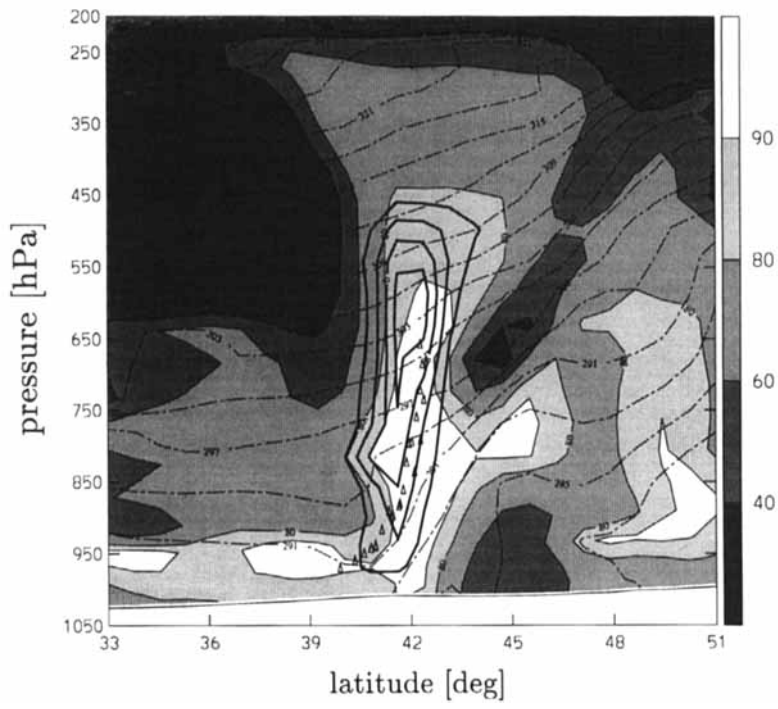

Figure 3. S-N oriented vertical section across the centre of the CET shown in Fig. 2(a) at longitude 21°W for 18 UTC 12 January 1993. Shown are the relative humidity field (shaded, see scale beside the panel), the potential temperature field (dashed lines, contour interval 3 K), the diagnosed diabatic heating rate (bold lines, contour interval 2 K/6 h, zero line omitted) and the tropopause (2 PVU contour, bold dashed line). Δ-symbols denote intersection points for trajectories of the CET that crossed this section in the time window ±1 hour.

forerunners and successors, influences cyclogenesis via the buoyancy anomaly generated by latent heat release near the storm centre and the structural and flow changes associated with its generation of anomalous potential vorticity. Thirdly, from a PV–θ perspective, the CET-related diabatically induced positive PV anomaly near the storm centre ranks in importance with the upper-level PV pattern and the surface θ distribution. However this diabatically induced anomaly differs significantly from the other two ingredients. It is neither quasi-conservative nor advected with the flow, but is generated *in situ* by the passage of the succession of CETs through the region of diabatic heating. For this case of 'steady condensation' the timescale for vertical advection of the saturated air parcels is comparable with the timescale of latent heating, leading to the generation of a positive PV anomaly close to the level of maximum diabatic heating (cf. Persson 1995; Stoelinga 1996). This is schematized in Fig. 4 where the process is also contrasted with the transient development of a vertically aligned PV-dipole due to an instantaneous cloud-diabatic effect (cf. Haynes and McIntyre 1987; Hoskins 1991).

(*b*) *Tracking of PV anomalies*

Current operational numerical weather prediction models and, in particular, high-resolution limited-area models generate a variety of subsynoptic-scale potential-vorticity structures. Examples include diabatically induced low-level anomalies ahead of surface fronts (see e.g. Hoskins and Berrisford 1988; Davis and Emanuel 1991; Reed *et al.* 1992; Neiman *et al.* 1993; Browning and Roberts 1994; Appenzeller and Davies 1996; Persson

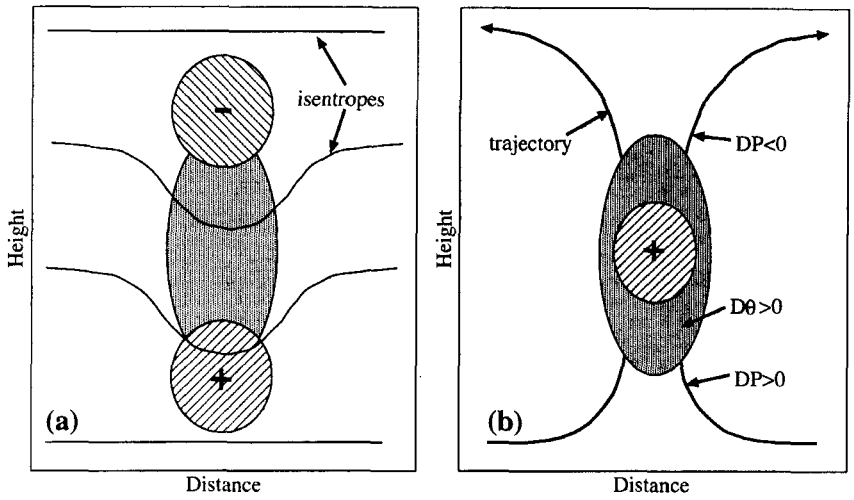

Figure 4. Schematic vertical cross-sections showing diabatically produced PV anomalies (hatched regions with a plus or minus sign) for the idealized cases of (a) 'impulsive diabatic heating', and (b) 'steady condensation' in a frontal zone. Shading indicates the region of diabatic heating. In (a) the solid lines are isentropes and in (b) the bold lines with arrows refer to air-parcel trajectories. $D\theta$ and DP denote material tendencies of potential temperature and potential vorticity, respectively.

1995), mesoscale structures associated with flow along or over mountains (Thorpe *et al.* 1993; Aebischer and Schär 1994), and elongated streamers of downward intruding stratospheric air (Appenzeller and Davies 1992; Browning 1993; Appenzeller *et al.* 1996).

These PV anomalies are often of dynamical significance and the issue of their formation and evolution are topics of interest in current research. Their analysis is rendered difficult by the lack of observational data-sets capable of resolving the system's subsynoptic space and time scales. Nevertheless consistency in the analysis and forecast of features of this kind offers the opportunity, albeit limited, to study their dynamics. It is in this context that two case-studies are provided here to illustrate the value of Lagrangian analysis.

(i) *First case.* This first case concerns two narrow low-level bands of positive PV anomalies that accompanied an Atlantic cyclogenesis event in late November 1992.

An indication of the character of the two bands can be gained from Fig. 5. This figure displays the potential vorticity and wind-vector distributions on a sequence of four six-hourly 850 hPa charts that culminate 18 hours before the time of maximum depth of the attendant cyclone. At 06 UTC 22 November the band labelled A is associated with a significant wind shift (it is in fact located within a frontal zone), and thereafter evolves as the centre of a frontal-wave cyclone (L) and by 00 UTC 23 November its PV pattern acquires an arched form around the low. In contrast band B is not associated with a wind-shift signal nor does it possess marked baroclinicity. This difference in the character of the bands is further emphasized in Fig. 6, which shows the distribution of PV, θ and humidity in a west–east section across the bands at 12 UTC 22 November. Band A forms a narrow and moist PV anomaly that extends up to 500 hPa, whilst band B is a broader and drier feature confined to low levels and distinguished by isentropic displacements in its vicinity that well up from below and bow down from above. The wind shift of band A and the isentropic pattern of B are consistent with the differing geometry of the accompanying PV patterns.

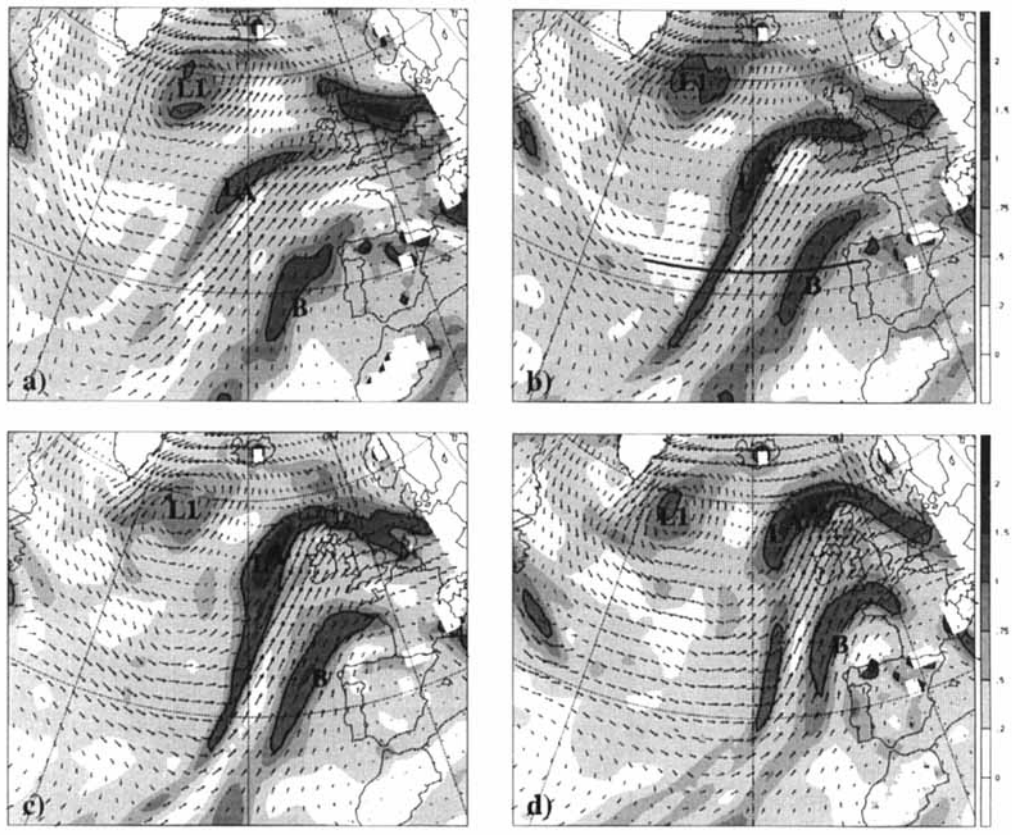

Figure 5. The potential vorticity (in PVU) and horizontal wind vectors on the 850 hPa surface at (a) 06 UTC 22 November, (b) 12 UTC 22 November, (c) 18 UTC 22 November and (d) 00 UTC 23 November 1992. The labels L and L1 denote the central position of two successively growing cyclones and the labels A and B mark the position of certain positive PV anomalies (see text for explanations). The bold line in panel (b) marks the location of the vertical section shown in Fig. 6.

For this case a succession of Lagrangian analyses were done for reference times corresponding to 06, 12, and 18 UTC 22 November and 00 UTC 23 November. In each case the *a priori* constraint imposed for bands A and B was for tropospheric PV values to be greater than 1.0 PVU. For each reference time both forward and backward tracking of bands A and B were performed for periods of the equivalent of 18 hours. The evolution of their mean height and potential-vorticity distribution is shown in Fig. 7. The succession of macro air parcels delineating the frontal band A are diabatically active with their PV values first increasing rapidly and then remaining constant, as the parcels ascend to mid-tropospheric levels, whereas band B is diabatically inactive and is essentially advected quasi-horizontally.

Thus the Lagrangian analysis pinpoints the markedly different dynamics of the two low-level PV anomalies. In particular it provides insight into the contribution of diabatic heating and advection to their origin and evolution. Note also that band A is a seminal element of the frontal-wave cyclogenesis and possesses many of the characteristics of the CET discussed in the previous subsection; whereas band B appears to be a dynamically passive and thermodynamically benign feature (although its isentropic signature generates ascent as it is advected along; hence it could trigger convective activity).

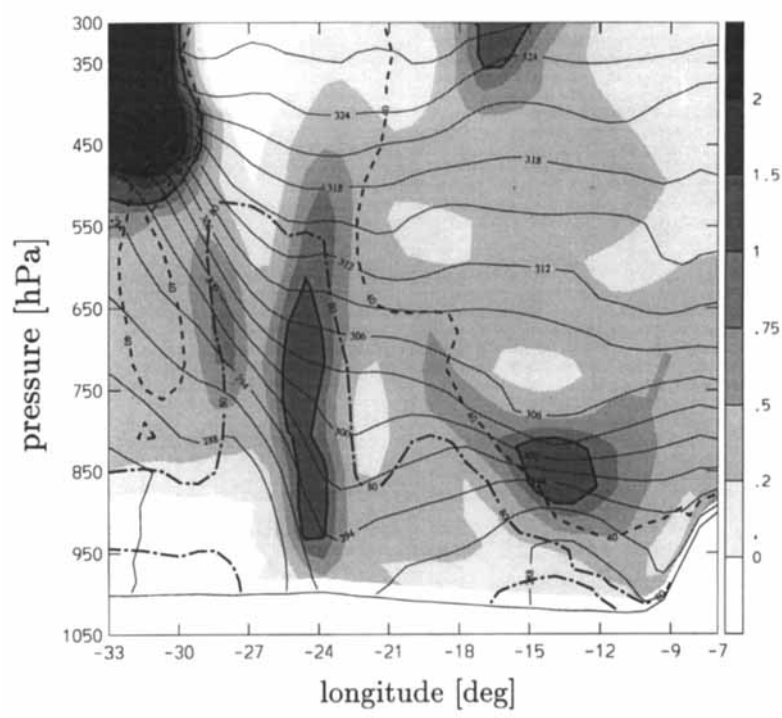

Figure 6. A west–east oriented vertical section at latitude 42°N across two low-level potential vorticity bands at 12 UTC 22 November 1992 (see Fig. 5(b)). Shown are the PV field (shaded, bold lines for 1 and 2 PVU), the potential temperature field (continuous lines, isoline spacing 3 K), and the relative humidity distribution (bold dash-dotted and dashed lines for values of 80% and 40%, respectively).

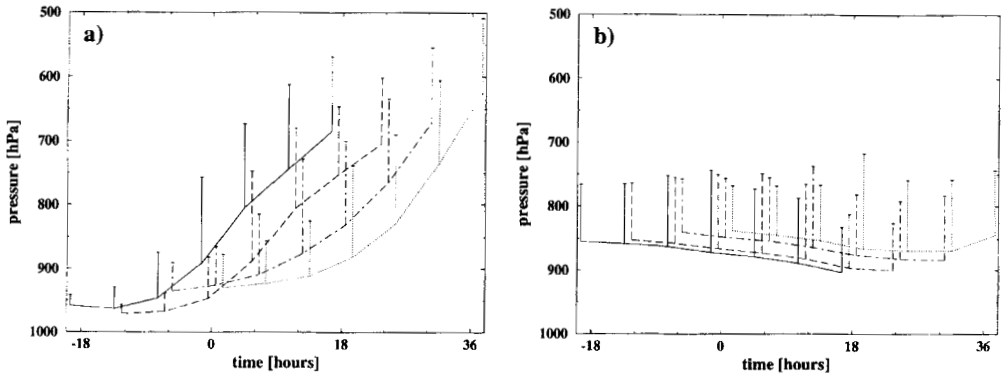

Figure 7. The mean pressure level of the forwards and backwards trajectories starting within the low-level PV anomalies (PV values > 1 PVU) at 06 UTC 22 November (continuous line), 12 UTC 22 November (dashed line), 18 UTC 22 November (dash-dotted line) and 00 UTC 23 November (dotted line) for (a) the anomaly A and (b) the anomaly B shown in Fig. 5. Time $t = 0$ corresponds to 06 UTC 22 November 1992. The vertical bars indicate the mean PV values at a time interval of 6 hours (the scale of 100 hPa corresponds to 1 PVU). For the sake of clarity the curves are slightly shifted relative to each other.

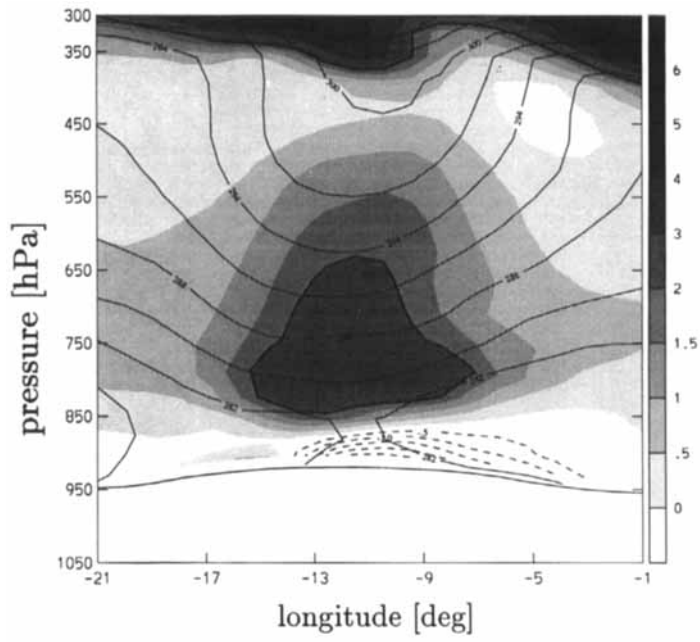

Figure 8. West–east oriented vertical section across the centre of the mature cyclone at latitude 62°N at 00 UTC 11 January 1993. Positive PV values are shaded (scale in PVU, the bold line denotes the 2 PVU contour), and negative PV values are indicated by dashed contours (isoline spacing 0.5 PVU). The potential temperature field is shown by continuous lines (isoline spacing 3 K).

(ii) *Second case.* The second case-study focuses on a negative low-level PV anomaly associated with a rapidly deepening Atlantic cyclogenesis that resulted in the Braer storm of January 1993. (For a synoptic overview of the storm see McCallum and Grahame 1993.)

The feature is evident in a west–east cross-section (Fig. 8) through the storm centre six hours after the time of minimum sea-level pressure at 00 UTC 11 January 1993. The section together with a contemporaneous north–south section (not shown) reveal strong quasi-symmetric potential-temperature and potential-vorticity signals. There is a warm core of diameter approximately 300 km extending up to a comparatively flat tropopause (cf. the 2 PVU iso-surface) at about 350 hPa, and a strong positive PV anomaly centred near 750 hPa (produced by condensational heating). The negative PV anomaly is confined to the lowest 50 hPa, has an amplitude of approximately 2.5 PVU, and is associated with an unstable thermal stratification. (The foregoing characteristics also featured in the 12 hours ECMWF forecast fields valid for the same time, although the amplitude of the negative PV anomaly was weaker by some 30%).

In this case the Lagrangian analysis was performed with the *a priori* constraint of a reference volume in which the PV values were below −1.0 PVU. Backwards tracking of this referenced macro air parcel (containing 33 trajectories) over a time period of 48 hours traced its location back to a cold region off Baffin Island, and its intermediate track was confined to the boundary layer below 900 hPa (see Fig. 9 and Table 2). The tabulated values indicate that the air parcel was warmed and moistened significantly as it traversed across comparatively warm ocean water. (The mean values of θ and θ_w, initially below 250 K, increased monotonically by more than 30 K, with a concomitant augmentation of the mean water-vapour content by a factor of 10). Inspection of the sensible and latent heat

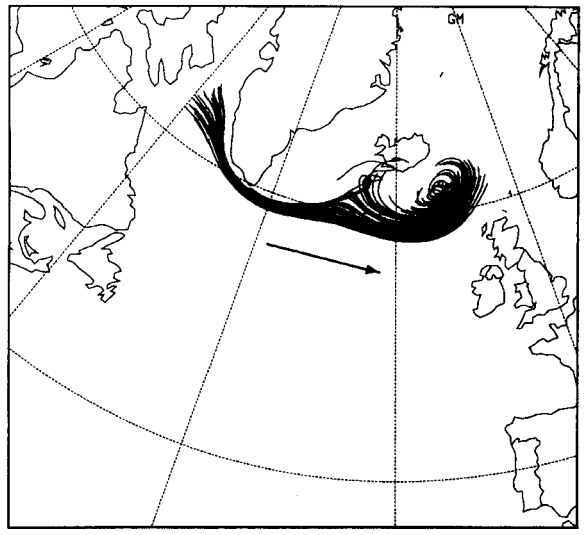

Figure 9. 48 hours backwards trajectories emanating at 00 UTC 11 January 1993 from the low-level region between Iceland and Scotland characterized by PV values below −1 PVU (cf. Fig. 8). The arrow indicates the direction of motion.

TABLE 2. TIME EVOLUTION OF THE MEAN CHARACTERISTIC VALUES OF THE BACKWARD TRAJECTORIES SHOWN IN FIG. 9.

t [h]	long	lat	p [hPa]	θ [K]	θ_w [K]	PV [PVU]	RH [%]	q [g kg^{-1}]
0	-9.9	62.2	915±14	282.4±1.1	278.7±0.9	-2.00±0.7	84± 8	4.1±0.4
-12	-24.5	59.8	942±13	276.3±3.4	272.5±3.3	0.01±0.3	57±10	2.2±1.1
-24	-35.1	60.0	948±22	269.5±2.4	267.4±1.9	-0.26±0.4	73±13	1.6±0.3
-36	-46.7	61.4	960±21	259.6±6.4	258.6±5.8	-0.46±1.0	79± 8	0.9±0.5
-48	-55.2	63.5	961±42	248.6±7.6	247.9±6.7	0.43±0.7	66± 8	0.3±0.3

Values are given every 12 hours of the trajectory integrations. Time $t = 0$ corresponds to 00 UTC 11 January 1993.

fluxes of the ECMWF fields at the −24 and −6 hour times (not shown) confirms that the location of the anomaly corresponded to regions of large positive sensible and latent heat fluxes.

This case-study of an unusual negative low-level PV anomaly within the core of an explosive cyclone indicates the geographical and thermodynamic history of the anomaly, and illustrates the method's potential to contribute to our understanding of non-standard dynamical features.

(*c*) *Trans-tropopause exchange*

Mid-latitude weather systems are frequently accompanied at tropopause levels by striking subsynoptic and mesoscale flow elements such as tropopause folds, filamentary streamers and cut-off lows. The study of these elements and, in particular, the assessment of their contribution to stratosphere–troposphere exchange (STE) has recently become the subject of renewed interest (see e.g. Bamber *et al.* 1984; Appenzeller and Davies 1992; Ancellet *et al.* 1994; Lamarque and Hess 1994; Browning and Reynolds 1994; Vaughan

et al. 1994; Appenzeller *et al.* 1996). Indications of STE in association with these features has been derived by various methods such as the co-examination of isentropic PV charts and water-vapour satellite imagery, the estimation of the instantaneous mass flux, and the application of the contour advection technique and trajectory calculations. Trajectory calculations were indeed used in some of the pioneering studies on the subject (Danielsen 1959; Staley 1960). Here we apply our Lagrangian technique and introduce selection criteria that yield direct information about the location and intensity of the exchange processes, the origin and destination of micro air parcels, and provide an indication of the non-conservative processes that accompany and are responsible for STE.

The approach adopted consists in defining the tropopause as the 2 PVU iso-surface and in identifying, for a stipulated space-time domain, the air parcels whose time traces signify a trans-tropopause migration from stratosphere to troposphere (S→T), and troposphere to stratosphere (T→S). To this end a two-step procedure is applied. First air parcels with a potential S→T (T→S) exchange are selected with the raw criterion that a parcel's initial potential vorticity is larger (smaller) than 2 PVU and that after 24 hours it is smaller (larger) than 2 PVU. In a second step the resulting set of selected trajectories are extended both forwards and backwards in time for the equivalent of five days. Significant S→T (T→S) exchange is then attributed to those air parcels whose extended trajectories reside entirely within the stratosphere (troposphere) during the first four days and within the troposphere (stratosphere) for the last four days. Thus this second and more severe criterion makes an allowance for the anticipated errors in estimating the PV in the vicinity of the richly structured extra-tropical tropopause and, concomitantly, it serves to distinguish between air parcels that transit one way across the tropopause from those that move to and fro across the interface.

This procedure is illustrated with a case-study based upon the same cyclogenetic event of January 1993 that was discussed earlier in section 3(a). The analysis is undertaken for three successive one-day time periods starting from 12 UTC 12 January. The stipulated spatial domain covers the entire region of cyclone development and covers approximatively 4000 × 2500 km, extending in the vertical from 550 to 250 hPa. Consider in turn the overall and the detailed characteristics of the deduced exchange. For S→T (T→S) exchange only 15-25% (5-15%) of the parcels that meet the first criterion also satisfy the second. This suggests a natural tendency for many air parcels to traverse only transiently across the tropopause on the timescale of less than four days rather than to undergo a sustained change. An estimate of the time evolution of the 'significant mass exchange' (i.e. based on air parcels that satisfy both criteria) is provided in Fig. 10. It shows a net S→T mass exchange for this event with a peak value of 2.35×10^{14} kg d^{-1} for the second 24-hour period—the time encompassing maximum storm intensification. This value compares reasonably with that derived by Lamarque and Hess (1994) for a cyclonic development along the east coast of the United States. Their calculations of the instantaneous mass flux yielded an estimate of 4.9×10^{14} kg in four days. Note however that their net exchange value is the residual of S→T and T→S values for the mass transfer that are both 4 to 5 times larger than those inferred here, and moreover that this factor is comparable to the ratio inferred by us for transient versus 'significant' mass exchange.

Consider now the spatial structure of the 'significant exchange' during the second time period. An indication of this is given in Fig. 11 which shows the position of the pertinent parcels at 00 UTC 14 January together with the pressure distribution at the tropopause level. Three regions of active exchange can be identified: one over north-western Europe associated with the cyclogenesis event considered in section 3(a), a second associated with a tropopause fold extending from Scandinavia to the south-east, and a third along the base and the downstream edge of a synoptic-scale trough over Russia. In the vicinity of the

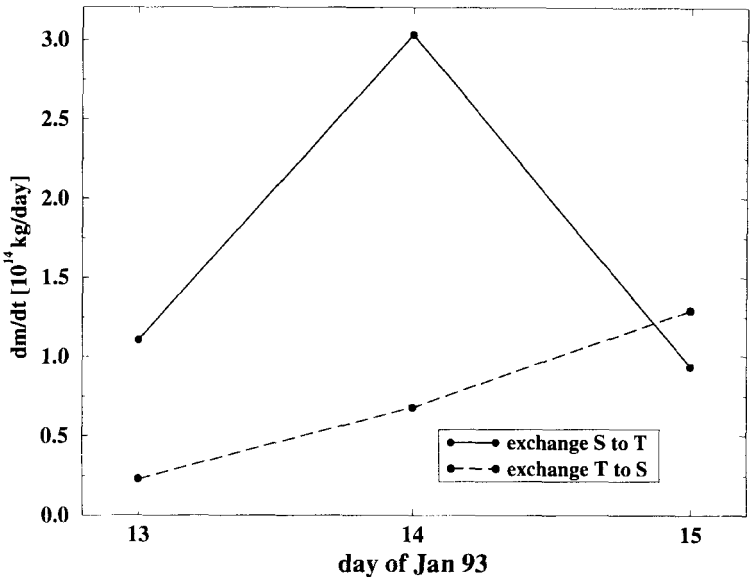

Figure 10. Estimates of the mass exchange from the stratosphere to the troposphere (continuous line) and from the troposphere to the stratosphere (dashed line) for three successive 24-hour time periods in kg d^{-1} (scaled by 10^{14}). The estimates are based upon the mass attributable to the 'significant' exchange particles only (see text for details).

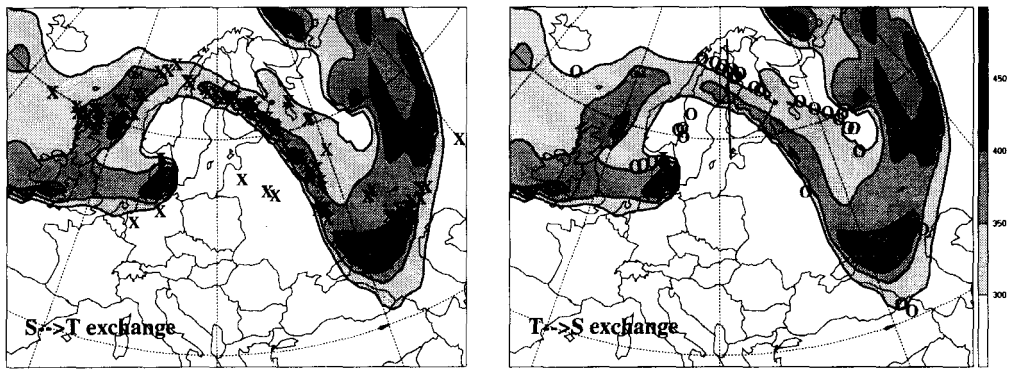

Figure 11. Position of the significant exchange particles at 00 UTC 14 January 1993 indicated by labels **X** for S→T exchange (left-hand panel) and **O** for T→S exchange (right-hand panel). Also shown is the pressure level of the tropopause, defined as the 2 PVU isosurface (shaded, bold isolines for 300, 350, 400 and 450 hPa). **L** denotes the position of a low-pressure system over Denmark (cf. Section 3a). The short straight line near the Baltic in the right-hand panel marks the location of the vertical section shown in Fig. 12.

surface cyclone there is a two-way exchange with T→S exchange in the ascending air near and to the north of the cyclone centre, and S→T exchange in the descending air to the rear of the surface low and its attendant cold front. In contrast, in the fold region there is T→S exchange on the northern edge of the fold and S→T exchange on its southern edge. The implied strong indirect transverse circulation with ascending motion within the weakly stratified air on the colder side of the tropopause fold is evident in Fig. 12. The third region with its matured trough is characterized exclusively by S→T exchange.

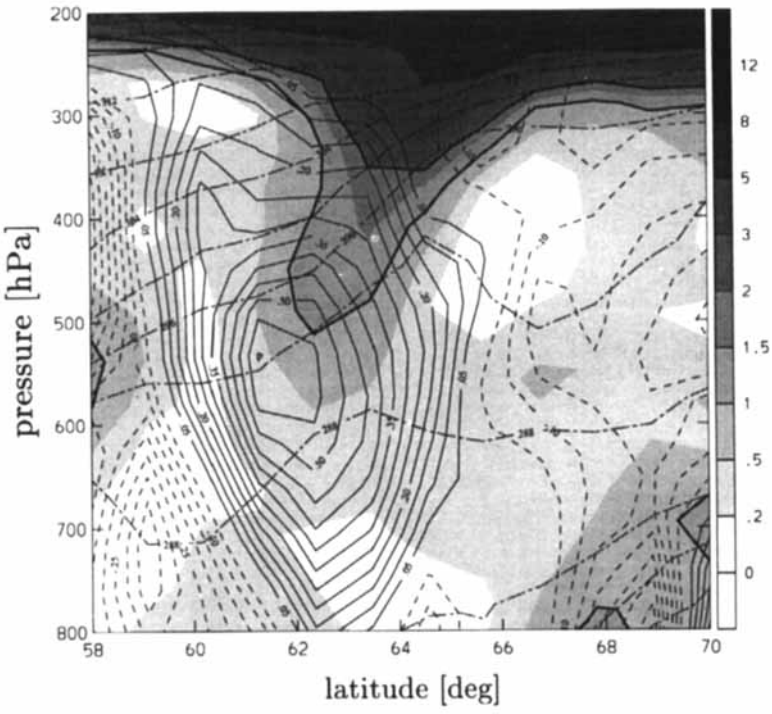

Figure 12. South–north oriented vertical section at 00 UTC 14 January across a tropopause fold structure at latitude 22°E. Shown are the potential vorticity field (shaded, see scale beside the panel, the 1 and 2 PVU contours are indicated by bold continuous lines), the potential temperature field (dash-dotted lines, contour interval 4 K), and the vertical-velocity field (dashed lines for upward motion, contour interval 0.05 Pa s^{-1}, the zero line is omitted).

From the Lagrangian characteristics of the S→T air parcels it can be inferred that five days before their tropopause transit they resided, typically, between 250 and 350 hPa at around latitude 60°N, and had mean PV and specific humidity values of, respectively, 4 ± 1 PVU and 0.01 g kg^{-1}. In the 5-day period following their tropopause transit their distribution differs significantly; 32% of the parcels remain north of latitude 50°N and above the 500 hPa level, 50% descend to the 500-800 hPa layer in mid latitudes, and the remaining 18% attain almost tropical latitudes near the Arabian Sea (Fig. 13), and descend to the 900 hPa level. The final potential vorticity and specific humidity values of these S→T parcels differ according to their destination and vary from 0–1 PVU and $0.05 - 7.0$ g kg^{-1}. Their potential temperature traces are broadly consistent with a radiative cooling rate of 1 K d^{-1}.

The T→S parcels had their origin within different vertical segments of the troposphere. About 25% ascended from below 800 hPa to the tropopause level with ascent rates much slower than for the CET discussed in section 3(a), although they experienced latent heat release. The traces of the remaining 75% indicated an essentially adiabatic ascent to the tropopause, which was traversed at around the 300 hPa level at latitudes 55°N to 65°N. After the traverse their mean motion was slowly downwards and to lower latitudes.

This case-study of stratosphere-to-troposphere mass exchange illustrates the potential of the Lagrangian analysis for identifying STE events, for estimating quantitatively the mass transfer and for shedding light on aspects of the origin and destination of the participating air parcels; and it reveals distinctive features such as the descent of mid-latitude stratospheric air to the sub-tropical boundary layer.

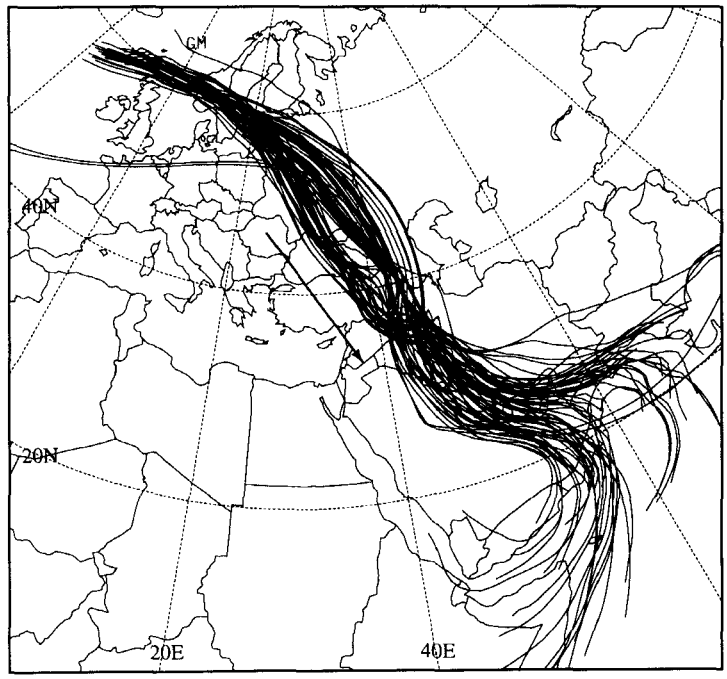

Figure 13. The path of the 'significant' S→T exchange particles for the 6-day period from 12 UTC 13 January to 12 UTC 19 January. Shown are only the trajectories which end to the south of latitude 25°N. The arrow indicates the direction of motion.

4. A SAMPLE CLIMATOLOGY OF CETs

An inevitable shortcoming of the case-study approach adopted in the previous section is its lack of generality. Thus, although additional case-studies reveal that a CET of the form identified in section 3(a) accompanies some other events of cyclogenesis, these studies do not suffice to indicate the representativity, frequency or the preferred geographical location (if any) of CETs. It is these issues that are the subject of the present section.

The method employed in the section 3(a) can be applied not only to investigate one particular event but also to provide a statistical analysis of the occurrence of events. To illustrate this point we examine the occurrence of moist ascending CETs (again selected using the criterion of a maximum decrease in specific humidity) for the northern hemisphere domain during the month of January 1993.

Sets of trajectories emanating from every gridpoint below the 800 hPa level in this domain were calculated at reference times separated by 12 hours. Each set was of 48 hours duration and this yielded a total of 55 overlapping time periods (i.e. the first period was from 00 UTC 1 January to 00 UTC 3 January, the second from 12 UTC 1 January to 12 UTC 3 January, etc. until the last period from 00 UTC 28 January to 00 UTC 30 January). CETs were then selected using the criteria of specific humidity decrease larger than (a) 12 g kg^{-1} and (b) 9 g kg^{-1} (only for the Atlantic region).

Figure 14 provides a composite view of the moist ascending CETs selected by the strong criterion (12 g kg^{-1}) with each curve now corresponding to the path marked out by the centre of a CET (the mean position of all trajectories), as opposed to the earlier depictions (e.g. Fig. 2) of the individual trajectories comprising a CET. On average, each CET curve represents about 100 trajectories—the minimum number was 20, and the ma-

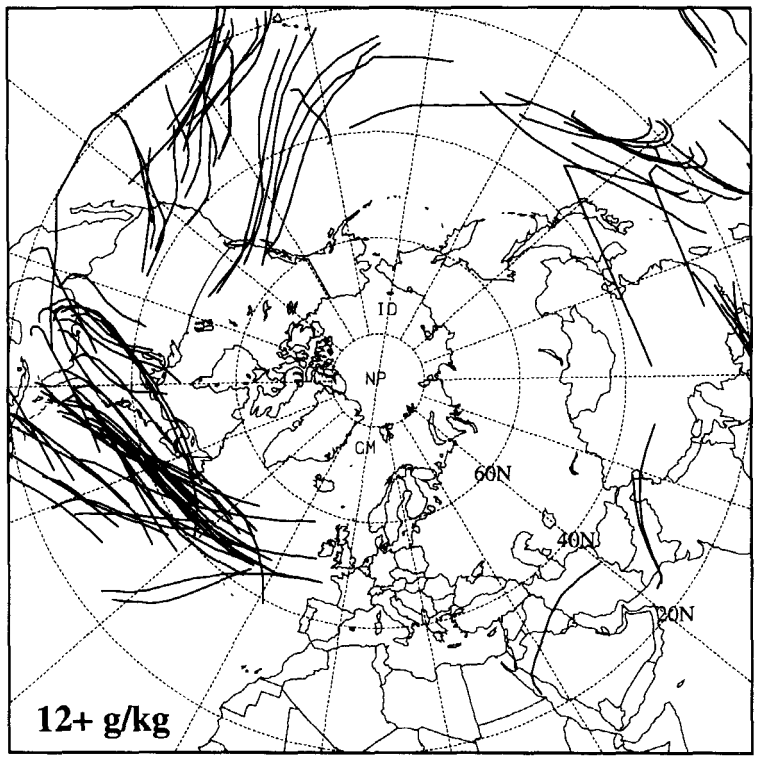

Figure 14. Composite view of the moist ascending CETs in January 1993 selected using the criterion of decrease in specific humidity greater than 12 g kg^{-1}. Note that in this diagram one line denotes the central path of an identified CET (i.e. not an individual trajectory as in Fig. 2).

jority of the CETs were again characterized by a high degree of coherence. In total, 85 CETs were identified which originated poleward of latitude 15°N. During the month the CETs occurred almost exclusively over the Pacific and Atlantic Oceans. In the Pacific there are two distinct groups: one originates at subtropical latitudes in the western Pacific and remains south of latitude 40°N; a second located in the eastern Pacific extends towards the western seaboard of North America. In the Atlantic the CETs originate predominantly in the Gulf of Mexico, the Caribbean and off the eastern seaboard of North America; they do not extend to the European mainland. Their average physical characteristics indicate an origin in the boundary layer and an ascent to upper-tropospheric levels (300–500 hPa). The time traces of θ, θ_w and PV confirm the significant contribution of diabatic processes: on the average a decrease of the water-vapour content by some 13 g kg^{-1}, an increase in potential temperature of more than 20 K, and an average PV trace with initial values typical of low tropospheric air (0.3 PVU), followed by an increase to 0.55 PVU within a diabatically active region, and a subsequent decrease to slightly below the original value.

A simple estimate can be made of the mean precipitation rate R associated with the identified CETs in the segment between latitudes 15°N and 60°N. This rate is equal to the ratio of the total water that condenses in any of the CETs to the area of that segment, and the former is estimated as the total number of trajectories (approx. 8900) times the mean decrease of water vapour (approx. 13 g kg^{-1}) times the typical volume of a low-level model grid box. The resulting estimate gives $R \approx 21$ mm for January 1993. This value is comparable with a typical climatological precipitation value for the mid latitudes (about

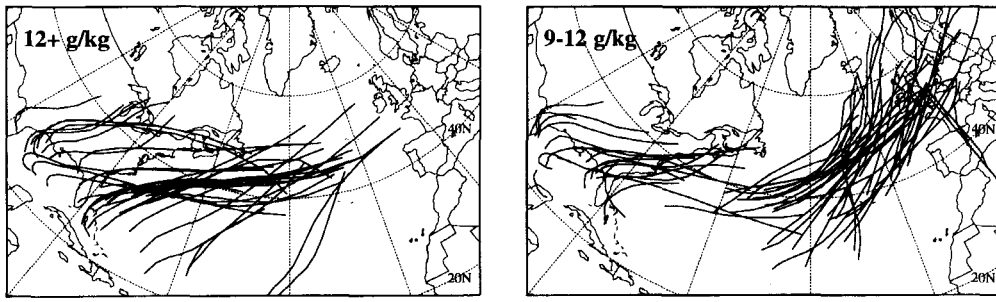

Figure 15. Composite view of the moist ascending CETs in January 1993 for the Atlantic region only. The left-hand panel corresponds to a detail of Fig. 14 (i.e. the CETs identified with the criterion of decrease in specific humidity greater than 12 g kg^{-1}), whereas the right-hand panel shows the CETs in the 9–12 g kg^{-1} category.

75 mm per month, cf. Fig. 9.17 from Wallace and Hobbs 1977), indicating that the CETs are indeed responsible for a significant portion of the mid-latitude precipitation.

Consider now the CETs in the Atlantic sector. Figure 15(b) pinpoints those that fall into the 9–12 g kg^{-1} category, i.e. the class of systems that includes the CET studied in section 3(a). These are also comparatively numerous (numbering 63, compared with 40 in the 12+ g kg^{-1} category), and their preferred source region is the eastern and mid Atlantic at about latitude 40°N. Thus it is systems in this category that are associated with the frontal-wave developments that influence much of the wintertime synoptic activity in the Atlantic–European sector and are the focus of the planned international FASTEX experiment (Fronts and Atlantic Storm-Track Experiment).

In summary this sample climatology of moist ascending CETs indicates that they are frequent features of the northern hemispheric wintertime circulation. They are linked to, and occur predominantly in the vicinity of, the dominant mid-latitude storm tracks of the northern hemisphere. Moreover the climatology provides some indication of a distinction between the CETs forming equatorwards of the storm track entrance and those that develop in mid track. Note also that some CETs, particularly the subtropical Pacific systems, are not associated with mid-latitude cyclones and occur within an environment of weak baroclinicity and pressure gradient and in the absence of striking upper-level signals. These subtropical CETs merit further study.

5. Discussion and further remarks

In this present study an objective method of Lagrangian analysis has been outlined, and various examples presented of its application in investigating the structure, dynamics and climatology of extratropical cyclones. The examples indicate that with this method it is possible to do the following:

(i) Identify objectively macro air-parcels (CETs) that, on the one hand, display a marked time coherency and, on the other hand, demarcate dynamically and thermodynamically active regions.
(ii) Trace the origin and help pinpoint the generation mechanisms of distinct subsynoptic-scale potential-vorticity anomalies.
(iii) Shed light on the evolution of flow features that can accomplish significant stratosphere–troposphere exchange.
(iv) Provide a climatology of the frequency and preferred geographical location for the occurrence of CETs.

Thus the approach, although limited by intrinsic shortcomings, has significant potential, and complements other diagnostic techniques. Here we comment briefly on the shortcomings, the potential and the complementarity of the technique.

The major shortcomings relate to the inadequate space–time resolution of the data fields currently available for the study of the richly structured synoptic/mesoscale flow structures, and the associated errors that can accrue in evaluating the Lagrangian time traces of the location and physical characteristics of the air parcels. These are trenchant caveats and they limit the credence that can be attached to the diagnosed finer-scaled characteristics of, for example, the moist ascending CETs. Another shortcoming stems from the adoption of a case-study approach. Analysis of several extratropical storm systems (Wernli 1995) reveals significant case-to-case variability in key features of the CETs—the location of their ascent relative to the developing cyclone, their curvature at upper levels and, to a lesser degree, of their coherence. Also, statistical analyses of CETs (cf. section 4) performed for another winter month (Wernli 1995) suggest significant interannual variability of the relative strength of CET activity in the Pacific versus the Atlantic sectors.

A pragmatic philosophy underlies the present study. The ECMWF analysis fields provide a data-base to initiate the study of Lagrangian flow structures, and the derived results are viewed as indicative of the existence and form of such features. In further mitigation we note that for most of the applications the results are not based upon the detailed characteristics of single trajectories but rather upon mean values of an ensemble of trajectories. (An exception is the consideration of stratosphere–troposphere exchange where the diagnosed across-tropopause mass transfer is sensitive to the accuracy of every single trajectory). Also, preliminary sensitivity studies undertaken with data derived from simulations with a high-resolution limited-area model indicate that the key Lagrangian features are not substantially changed by an increase in the spatial and temporal resolution of the available data. However, comparison with a fine-scale observational data-set (when available) would provide a more rigorous test.

An indication of the potential of the Lagrangian technique was provided by the examples considered in section 3. These were chosen to be illustrative rather than exhaustive. The methodology can also be used for a range of other studies. It can be used to examine descending airflows, and CETs at different phases of cyclogenesis and for markedly different events of cyclogenesis. Such studies would provide information on the co-development and the possible in-phase conjunction of PV anomalies at peak cyclogenesis, and thereby conceivably lead to a classification of cyclogenesis based upon the character of the CETs. The method can also be readily deployed to establish the CET climatology at different seasons and years, and to examine the relationship of CETs to conventional storm tracks. It can also be used to extend or refine previous trajectory-based studies on the influence of orography (cf. Steinacker 1984; Jäger 1992; Rössler *et al.* 1992), and nature of flow in the middle atmosphere (e.g. Sutton 1994).

In terms of complementarity the results derived with the present approach relate to several Lagrangian-like features diagnosed with other analysis techniques. First note that a coherent ensemble of trajectories (a CET) does not equate directly to the notion of 'conveyor-belts'. However the space–time form of a succession of CETs would not only illustrate the structural changes of CETs during the evolution of a mid-latitude cyclone, but would also bear a close connection to the conveyor-belt notion and indeed test the fidelity of that notion. Likewise the present approach can provide a Lagrangian-based view of so-called 'tropospheric rivers'—filamentary structures in the vertically integrated water vapour flux field (Newell *et al.* 1992). Both these issues are covered by Wernli (1996).

The present approach is also closely linked to the PV-perspective of atmospheric flow. For some of the examples considered in section 3 the selection criteria were formulated

explicitly in terms of potential vorticity and the results evaluated in terms of PV (and potential temperature). These examples shed light on the key dynamical elements of the PV perspective. In particular, evidence was given relating to the generation of diabatically induced PV anomalies in the troposphere and the evolution and fate of pre-existing PV anomalies at tropopause levels. Thus the present Lagrangian-based analysis technique complements the PV perspective and, concomitantly, provides a time-integrated depiction of the structure and dynamics of key elements of mid-latitude cyclogenesis.

ACKNOWLEDGEMENTS

The enthusiastic support of Christoph Schär has been very helpful in particular during the early phase of this project, and the comments and queries of Keith Browning were most instructive. Helpful comments on an earlier draft of the manuscript were also received from Christoph Appenzeller, Toby Carlson, Mike Pedder, Richard Reed and Volkmar Wirth. The help of Daniel Lüthi and David Bresch with aspects of the data acquisition and graphics is also appreciated. Parts of the diagnostic computations and visualizations were done with the IVE graphics package developed at the University of Washington. The help of the Swiss Meteorological Office (SMA) is gratefully acknowledged for granting access to the ECMWF data archive.

REFERENCES

Aebischer, U. and Schär, C. 1994 High resolution simulation of low-level flow features in the Alpine region. *Ann. Meteorol.*, **30,** 125–128

Ancellet, G., Beekmann, M. and Papayannis, A. 1994 Impact of a cutoff low development on downward transport of ozone in the troposphere. *J. Geophys. Res.*, **99,** 3451–3468

Appenzeller, C. and Davies, H. C. 1992 Structure of stratospheric intrusions into the troposphere. *Nature*, **358,** 570–572

1996 PV morphology of a frontal-wave development. *Meteorol. Atmos. Phys.*, **58,** 21–40

Appenzeller, C., Davies, H. C. and Norton, W. A. 1996 Fragmentation of stratospheric intrusions. *J. Geophys. Res.*, **101,** 1435–1456

Bader, M. J., Forbes, G. S., Grant, J. R., Lilley, R. B. .E. and Waters, A. J. (Eds.) 1995 *Images in weather forecasting*, Cambridge University Press

Bamber, D. J., Healey, P. G. W., Jones, B. M. R., Penkett, S. A., Tuck, A. F. and Vaughan, G. 1984 Vertical profiles of tropospheric gases: Chemical consequences of stratospheric intrusions. *Atmos. Environ.*, **18,** 1759–1766

Berrisford, P. 1988 'Potential vorticity in extratropical cyclones.' Ph. D. Thesis, Univ. of Reading

Browning, K. A. 1990 Organisation of clouds and precipitation in extratropical cyclones. Pp. 129–154 in *Extratropical cyclones. The Erik Palmen Memorial Volume.* Eds. C. Newton and E. O. Holopainen. American Meteorological Society, Boston

1993 Evolution of a mesoscale upper tropospheric vorticity maximum and comma cloud from a cloud-free two-dimensional potential vorticity anomaly. *Q. J. R. Meteorol. Soc.*, **119,** 883–906

1995 'Mesoscale aspects of extratropical cyclones: an observational perspective'. Intern. Rep. 44. Joint Centre for Mesoscale Meteorology, Reading UK

Browning, K. A. and Mason, J. 1981 Air motion and precipitation growth in frontal systems. *Pure Appl. Geophys.*, **119,** 577–593

Browning, K. A. and Reynolds, R. 1994 Diagnostic study of a narrow cold-frontal rainband and severe winds associated with a stratospheric intrusion. *Q. J. R. Meteorol. Soc.*, **120,** 235–257

Browning, K. A. and Roberts, N. M. 1994 Structure of a mid-latitude cyclone before occlusion. *Q. J. R. Meteorol. Soc.*, **120,** 1535–1557

Carlson, T. N. 1991 *Mid-latitude weather systems.* Harper Collins Academic

Danielsen, E. F. 1959 The laminar structure of the atmosphere and its relation to the concept of a tropopause. *Arch. Met. Geoph. Biokl.*, **A11,** 293–332

1980 Stratospheric source for unexpectedly large values of ozone measured over the pacific ocean during Gametag, August 1977. *J. Geophys. Res.*, **85,** 401–412

Davies, H. C. 1994 Theories of frontogenesis. Pp. 182–192 in *Proc. int. symp. life cycles of extratropical cyclones*, Vol. I. Eds. S. Grønås and M. A. Shapiro, Bergen, Norway

Davis, C. A. and Emanuel, K. A. 1991 Potential vorticity diagnostics of cyclogenesis. *Mon. Weather Rev.*, **119,** 1929–1953

Doty, K. G. and Perkey, D. J. 1993 Sensitivity of trajectory calculations to the temporal frequency of wind data. *Mon. Weather Rev.*, **121,** 387–401

Dove, W. H. 1840 *Über das Gesetz der Stürme*, Berlin (4. Ausgabe 1873)

Fitzroy, R. 1863 *The Weather Book. A Manual of Practical Meteorology*, London (Second Edition)

Green, J. S. A., Ludlam, F. H. and McIlveen, J. F. R. 1966 Isentropic relative-flow analysis and the parcel theory. *Q. J. R. Meteorol. Soc.*, **92,** 210–219

Harrold, T. W. 1973 Mechanisms influencing the distribution of precipitation within baroclinic disturbances. *Q. J. R. Meteorol. Soc.*, **99,** 232–251

Haynes, P. H. and McIntyre, M. E. 1987 On the evolution of isentropic distributions of potential vorticity in the presence of diabatic heating and frictional or other forces. *J. Atmos. Sci.*, **44,** 828–841

Hoskins, B. J. 1991 Towards a PV–θ view of the general circulation. *Tellus*, **43AB,** 27–35

Hoskins, B. J. and Berrisford, P. 1988 A potential vorticity perspective of the storm of 15–16 October 1987. *Weather*, **43,** 122–129

Hoskins, B. J., McIntyre, M. E. and Robertson, A. W. 1985 On the use and significance of isentropic potential vorticity maps. *Q. J. R. Meteorol. Soc.*, **111,** 877–946

Jäger, A. 1992 'Isentrope Trajektorien und ihre Anwendung auf das Konzept der potentiellen Vorticity bei orographisch induzierten Lee-Zyklogenesen.' Diploma thesis. University of Innsbruck

Kuo, Y.-H., Reed, R. J. and Low-Nam, S. 1992 Thermal structure and airflow in a model simulation of an occluded marine cyclone. *Mon. Weather Rev.*, **120,** 2280–2297

Lamarque, J. F. and Hess, P. G. 1994 Cross-tropopause mass exchange and potential vorticity budget in a simulated tropopause folding. *J. Atmos. Sci.*, **51,** 2246–2269

Mass, C. F. and Schultz, D. M. 1993 The structure and evolution of a simulated midlatitude cyclone over land. *Mon. Weather Rev.*, **121,** 889–917

McCallum, E. and Grahame, N. S. 1993 The Braer storm—10 January 1993. *Weather*, **48,** 103–107

Namias, J. 1939 The use of isentropic analysis in short term forecasting. *J. Aeronaut. Sci.*, **6,** 295–298

Neiman, P. J., Shapiro, M. A. and Fedor, L. S. 1993 The life cycle of an extratropical marine cyclone. Part II: Mesoscale structure and diagnostics. *Mon. Weather Rev.*, **121,** 2177–2199

Newell, R. E., Newell, N. E., Zhu, Y. and Scott, C. 1992 Tropospheric rivers?—A pilot study. *Geophys. Res. Lett.*, **12,** 2401–2404

Palmén, E. 1953 'On the dynamics of cold air outbreaks in the westerlies.' Univ. Chicago, Dept. Meteorol., Off. Naval Res., final rep. general circ. project

Persson, P. O. G. 1995 Simulations of the potential vorticity structure and budget of FRONTS 87 IOP 8. *Q. J. R. Meteorol. Soc.*, **121,** 1041–1081

Petterssen, S. 1956 *Weather analysis and forecasting. Vol. I, Motion and motion systems*. McGraw-Hill

Reed, R. J., Stoelinga, M. T. and Kuo, Y.-H. 1992 A model-aided study of the origin and evolution of the anomalously high potential vorticity in the inner region of a rapidly deepening marine cyclone. *Mon. Weather Rev.*, **120,** 893–913

Rossby, C.-G. 1945 The scientific basis of modern meteorology. Pp. 501–529 in *Handbook of meteorology*. Eds. F. A. Berry, E. Bollay and N. R. Beers, McGraw-Hill

Rossby, C.-G. and collaborators 1937 Isentropic analysis. *Bull. Am. Meteorol. Soc.*, **18,** 201–209

Rössler, C. E., Paccagnella, T. and Tibaldi, S. 1992 A three-dimensional atmospheric trajectory model: Application to a case study of Alpine lee cyclogenesis. *Meteorol. Atmos. Phys.*, **50,** 211–229

Schär, C. and Wernli, H. 1993 Structure and evolution of an isolated semi-geostrophic cyclone. *Q. J. R. Meteorol. Soc.*, **119,** 57–90

Seibert, P.	1993	Convergence and accuracy of numerical methods for trajectory calculations. *J. Appl. Meteor.*, **32,** 558–566
Shapiro, M. A. and Keyser, D.	1990	Fronts, jet streams and the tropopause. Pp. 167–191 in *Extratropical cyclones. The Erik Palmen Memorial Volume.* Eds. C. Newton and E. O. Holopainen. American Meteorological Society, Boston
Shaw, W. N.	1903	The meteorological aspects of the storm of February 26–27, 1903. *Q. J. R. Meteorol. Soc.*, **29,** 233–262
Shaw, W. N. and Lempfert, R. G. K.	1906	The life history of surface air currents. A study of the surface trajectories of moving air. *M. O.* **174** (Available in the National Meteorological Library, Bracknell, UK)
Simmons, A. J.	1991	Development of a high resolution, semi-Lagrangian version of the ECMWF forecast model. Pp. 281–324 in *Numerical methods in atmospheric models, Vol. II.* ECMWF, Reading UK
	1994	Numerical simulations of cyclone life cycles. Pp. 149–160 in *Proc. int. symp. life cycles of extratropical cyclones, Vol. I.* Eds. S. Grønås and M. A. Shapiro, Bergen, Norway
Staley, D. O.	1960	Evaluation of potential vorticity changes near the tropopause and the related vertical motions, vertical advection of vorticity, and transfer of radioactive debris from stratosphere to troposphere. *J. Meteorol.*, **17,** 591–620
Steinacker, R.	1984	Airmass and frontal movement around the Alps. *Riv. Meteorol. Aeron.*, **XLIII,** 85–93
Stoelinga, M. T.	1996	A potential vorticity-based study of the role of diabatic heating and friction in a numerically simulated baroclinic cyclone. *Mon. Weather Rev.*, **124,** 849–874
Sutton, R.	1994	Lagrangian flow in the middle atmosphere. *Q. J. R. Meteorol. Soc.*, **120,** 1299–1321
Thorpe, A. J.	1994	Dynamics of mesoscale sub-structures at fronts. Pp. 220–228 in *Proc. int. symp. life cycles of extratropical cyclones, Vol. I.* Eds. S. Grønås and M. A. Shapiro, Bergen, Norway
Thorpe, A. J., Volkert, H. and Heimann, D.	1993	Potential vorticity of flow along the Alps. *J. Atmos. Sci.*, **50,** 1573–1590
Vaughan, G., Price, J. D. and Howells, A.	1994	Transport into the troposphere in a tropopause fold. *Q. J. R. Meteorol. Soc.*, **120,** 1085–1103
Wallace, J. M. and Hobbs, P. V.	1977	*Atmospheric science. An introductory survey*, Academic Press, New York
Wernli, H.	1995	'Lagrangian perspective of extratropical cyclogenesis.' Ph. D. thesis. Dissertation Nr. 11016 ETH Zürich
	1997	A Lagrangian-based analysis of extratropical cyclones. II: A detailed case study. *Q. J. R. Meteorol. Soc.*, **123,** (in press)
Whitaker, J. S., Uccellini, L. W. and Brill, K. F.	1988	A model-based diagnostic study of the rapid development phase of the President's Day cyclone. *Mon. Weather Rev.*, **116,** 2337–2365
Young, M. V., Monk, G. A. and Browning, K. A.	1987	Interpretation of satellite imagery of a rapidly deepening cyclone. *Q. J. R. Meteorol. Soc.*, **113,** 1089–1115